NanoImpact 14 (2019) 100159

Contents lists available at ScienceDirect

NanoImpact

journal homepage: www.elsevier.com/locate/nanoimpact

Release of radiolabeled multi-walled carbon nanotubes (^{14}C-MWCNT) from epoxy nanocomposites into quartz sand-water systems and their uptake by *Lumbriculus variegatus*

Michael Patrick Hennig[a,*], Hanna Maja Maes[a], Richard Ottermanns[a], Andreas Schäffer[a], Nina Siebers[b,c]

[a] Institute for Environmental Research, RWTH Aachen University, Worringerweg 1, 52074 Aachen, Germany
[b] Forschungszentrum Jülich GmbH, Agrosphere (IBG-3) Institute of Bio- and Geosciences, Wilhelm-Johnen-Straße, 52425 Jülich, Germany
[c] Forschungszentrum Jülich GmbH, Ernst Ruska-Centre for Microscopy and Spectroscopy with Electrons (ER-C), Wilhelm-Johnen-Straße, 52425 Jülich, Germany

A B S T R A C T

Once plastic products containing multi-walled carbon nanotubes (MWCNT) are disposed, UV-light exposure may destabilize their structural integrity, leading to a release of MWCNT into the environment that can possibly be taken up by organisms and cause adverse effects. The aim of this study was to quantify the released amount of embedded ^{14}C–MWCNT epoxy (E) nanocomposites. Furthermore, bioaccumulation of the released material was investigated in *Lumbriculus variegatus*.

The release of radioactivity (RA) from irradiated (+SSR) E/^{14}C-MWCNT composites was quantified after a series of mechanical treatments and in a quartz sand-water system. Non-irradiated composites served as control group (-SSR). Unlabeled ± SSR-nanocomposites were analyzed by means of electron microscopy. The exposure of blackworms to the released material and the amount of RA in the water phase, the quartz sand, and the faeces was quantified.

About 0.1% of the embedded RA was released from +SSR-nanocomposites by mechanical treatment and exposure in the quartz sand-water system, which was about 23 times higher compared to -SSR composites. This corresponds to around 3 mg ^{14}C-MWCNT m^{-2} for both approaches. Based on the released mass per composite area, +SSR plates set free a 50-fold higher amount of RA. A detectable amount of 7.3 ± 1.8 ng of ^{14}C-MWCNT was also found in the water phase of the quartz sand-water systems. Electron microscopy revealed an enhanced surface degradation of the composites after SSR and mechanical treatments. Released polymer particles also contained protruding MWCNT. An amount of 2.4 ± 1.8% of released RA was taken up by blackworms after 2 d and about 66% of ingested material was eliminated again after 24 h.

The results of this study show that SSR leads to an enhanced release of mostly E-polymer associated MWCNT from nanocomposites that are bioavailable for sediment-dwelling organisms, although the absolute amount of released material is low. Follow-up studies examining toxicological effects after uptake are essential for the environmental risk assessment of MWCNT and E/MWCNT-composites.

1. Introduction

From 1950 to 2014 the worldwide yearly amount of plastic products increased gradually from 1.5 to 311 megatons (Ivleva et al., 2017). Multi-walled carbon nanotubes (MWCNT) can be easily embedded in such plastic polymers. This incorporation of MWCNT as additives enhances various properties of composites compared to neat plastic materials. (Wetzel et al., 2003; Sulong et al., 2006; Hollertz et al., 2011; Jackson et al., 2016). For the production of nanocomposites, a wide range of plastic polymer can be used, such as polyamide, polystyrene, polyethylene, polypropylene, polycarbonate, polyurethane, or epoxy resin (E). Usually, such plastic materials undergo life-cycle processes from synthesis of the polymers and MWCNT to their use and finally their disposal (Nowack et al., 2013; Wohlleben et al., 2016).

A low risk for human and the environment is expected from nanocomposite products as long as MWCNT remain integrated in the surrounding matrix polymer during their complete life-cycle (Wohlleben et al., 2011b; Hirth et al., 2013). Recent studies revealed that degradation of MWCNT embedded nanocomposites leads to an enhanced release of polymer fragments with containing and protruding MWCNT (Hirth et al., 2013; Petersen et al., 2014; Schlagenhauf et al., 2015b; Rhiem et al., 2016; Neubauer et al., 2017). During the consumer use of a product mechanical stress as well as weathering processes will take place in the environment, e.g., temperature, moisture, leaching, salinity, or solar irradiation after disposal, which might cause the material to release low amounts of MWCNT (Harper et al., 2015).

As such products reach their end-of-life, they are usually disposed or incinerated. About 69% of plastic waste is recovered through recycling and energy recovery processes; the remaining part is stored in landfills (Ivleva et al., 2017). By transportation through winds or carelessly

* Corresponding author at: Worringerweg 1, 52074 Aachen, Germany.
E-mail address: Michael.Hennig@rwth-aachen.de (M.P. Hennig).

https://doi.org/10.1016/j.impact.2019.100159
Received 14 February 2019; Received in revised form 4 April 2019; Accepted 10 April 2019
Available online 19 April 2019

disposed waste, neat and MWCNT containing plastic debris finally enter the terrestrial and aquatic environment (Primpke et al., 2017; Nowack and Mitrano, 2018). This waste is then exposed to different environmental weathering processes, e.g., temperature or UV-light, causing a steady degradation of the plastic polymer and thus a potential release of MWCNT.

Many studies already described that UV-irradiation increases the degradation of several MWCNT containing plastic polymers, resulting in a release of material fragments containing and protruding MWCNT as well as single MWCNT (Hirth et al., 2013; Ging et al., 2014; Kingston et al., 2014; Petersen et al., 2014; Schlagenhauf et al., 2015b; Wohlleben et al., 2016; Koivisto et al., 2017; Nguyen et al., 2017). UV-degradation of composite surface polymer causes a delamination of a 2.5 µm thick layer (Schlagenhauf et al., 2015b). Furthermore, a dense, entangled MWCNT network structure is formed on the surface, though no release of MWCNT is detected (Nguyen et al., 2017). Combination of high-shear wear and UV-degradation leads to a release of free MWCNT in order of mg m^{-2} $year^{-1}$ (Hirth et al., 2013). However, in all these studies the release of MWCNT from nanocomposites could not be directly quantified. Only Rhiem et al. (2016) presented a study in which an 80-fold stronger release of MWCNT from irradiated polycarbonate/MWCNT was exactly determined by using ^{14}C-labeled MWCNT. However, experimental data for release rates from different nanocomposites types are still missing (Rhiem et al., 2016) but urgently required, although simulated release scenarios predict a potential release of MWCNT during the whole life cycle of a nanocomposite (Eckelman et al., 2012; Nowack et al., 2013; Caballero-Guzman and Nowack, 2016; Sun et al., 2017).

Until now, no release behaviour or fate of (weathered and degraded) polymer fragments and single MWCNT from nanocomposites into sediments and soils was assessed. One possible pathway of the released polymer fragments and single MWCNT leads directly into different aquatic and terrestrial biotopes without a cleaning procedure by a treatment plant, e.g., lakes, rivers, oceans, or soil (Nowack et al., 2013; Caballero-Guzman and Nowack, 2018). Depending on the polymer material, polymer density and on the photo-oxidation processes, fragments either tend to remain in the aqueous phase or rapidly deposit in sediments, that usually act as a sink for carbonaceous, hydrophobic matter like MWCNT (Schierz et al., 2014; Eerkes-Medrano et al., 2015; Besseling et al., 2017b; Kooi et al., 2018). It can be hypothesized that due to rapid surface polymer UV-degradation the release of MWCNT and polymer fragments into sediments is enhanced by additional mechanical abrasion under environmental conditions than for non-irradiated samples. The released material is expected to be photo-oxidized by UV-light on the MWCNT- and fragment surfaces rendering the particles more hydrophilic.

To the best of our knowledge no ecotoxicological studies with released material in environmental media from (weathered) MWCNT nanocomposites are available. MWCNT and micro- and nanoplastics alone may cause negative effects on aquatic and terrestrial organisms and can be ingested as well (Maes et al., 2014; Rhiem et al., 2015; Kesy et al., 2016; Besseling et al., 2017a; Hurley et al., 2017). Even though bioaccumulation of MWCNT, micro-, and nanoplastics alone is assumed to be low in aquatic and terrestrial biota (Duis and Coors, 2016; Bjorkland et al., 2017), the increasing production of MWCNT enhanced plastic products will further burden the environment while ecotoxicological data are urgently required. It can be assumed that these released materials are potentially ingested by aquatic and benthic biota, eventually causing negative effects.

This study aimed at a comparison and quantification of released MWCNT amounts from simulated sunlight irradiated and non-irradiated E/MWCNT nanocomposites (i) after a series of mechanical treatments (ii) in quartz sand-water systems. Furthermore, (iii) uptake and excretion by a sediment-dwelling organism was quantified.

2. Materials and methods

2.1. Synthesis of ^{14}C-labeled MWCNT

Radiolabeled MWCNT (^{14}C-MWCNT) were synthesized by catalytic chemical vapour deposition with the help of Bayer Technology Services GmbH (BTS, Leverkusen, Germany). Details on the synthesis can be found in Maes et al. (2014) and Rhiem et al. (2015). The radioactive label was incorporated in the graphene walls of the nanotubes with a specific RA of 1.9 MBq/ mg ^{14}C-MWCNT. ^{14}C-MWCNT contained 3–15 walls with an inner diameter of 4 nm, an outer diameter of 5–20 nm, and a length of ≥1000 nm. After washing the product with 12.5% hydrochloric acid, the carbon purity of synthesized ^{14}C-MWCNT was above 95%. This means, that all ^{14}C-radiolabeled (and non-labeled, ^{12}C) carbon atoms belongs to these 95%. It is possible, that some part of the impurities also contains ^{14}C, which might be released, but since the untreated (control) MWCNT did release only tiny amounts compared to the treated MWCNT, it can be assured, that release is due to degradation of the polymer matrix. In addition, impurity of MWCNT includes residual inorganic contaminants from the catalysts used for synthesis of MWCNT (personal information from the producer). Such impurities do not contain ^{14}C. For production of epoxy nanocomposites with non-radioactive MWCNT (E/MWCNT), unlabeled MWCNT (Baytubes® C150P) were provided by BTS. These MWCNT were produced by the same synthetic procedure on a larger scale. A comparison of radiolabeled and unlabeled MWCNT by electron microscopy revealed same structural characteristics (Rhiem et al., 2016).

2.2. Production of E/MWCNT nanocomposites

The E/MWCNT nanocomposites were produced with an MWCNT percentage of 0.25% (w/w). Eleven grams of E/MWCNT raw material were produced for all plates. In the first step 8.7 g of epoxy resin (Huntsman Advanced Materials, Switzerland) were mixed with 5 g ethanol (≥99.8%) at 80 °C to obtain a fluent and smooth mixture. Simultaneously, 27.5 mg of MWCNT (Baytubes C150 P) were homogenously dispersed in 15 g ethanol by using an ultrasonic disintegrator with a microtip, twice for 10 min (Sonopuls HD 2070, 70 W, pulse: 0.2 s, pause: 0.8 s). This dispersion was then slowly dropped into the resin and the mixture was stirred until the ethanol was evaporated completely. During stirring the resin containing MWCNT was ultrasonicated four times for 10 min using the same settings (see SI).

Subsequently, 2.3 g hardener, consisting of 100 parts Aradur 1571 and 13 parts of Accelerator 1573 (Huntsman Advanced Materials, Switzerland), were added into the resin under stirring (ratio 10:2.6 resin:hardener). The raw bulk material was portioned into small Teflon moulds (Ø 18 mm, Fig. A1 B) forming composite plates with a weight of 300 to 400 mg. In the last step the plates were dried at 80 °C for 1 h and subsequently heated at 120 °C for at least 2 h. The product was briefly cleaned in ethanol and stored in the dark until the beginning of the experiments (Fig. A1 C) Description of the mean diameter and weight of the plates can be found in the SI. Based on the assumption that ^{14}C-MWCNT are homogenously distributed within the composite polymer, the initially embedded amount of RA was calculated by the amount of ^{14}C-MWCNT used for production of the composite plates (0.25% w/w) multiplied by the actual weight of each plate.

2.3. Weathering of nanocomposites by simulated sunlight radiation

One part of the produced E/MWCNT composites (radiolabeled and unlabeled) was subsequently weathered by simulated sunlight radiation (SSR) using a weathering testing apparatus with slight changes according to ISO 3892-2:2006 (Suntest™ CPS+, Altas Material Testing Technology, Germany, standard black temperature 65 °C, dry conditions). An air-cooled xenon lamp (1500 W) with a daylight UV filter producing light with a wavelength range of 300 to 400 nm irradiated

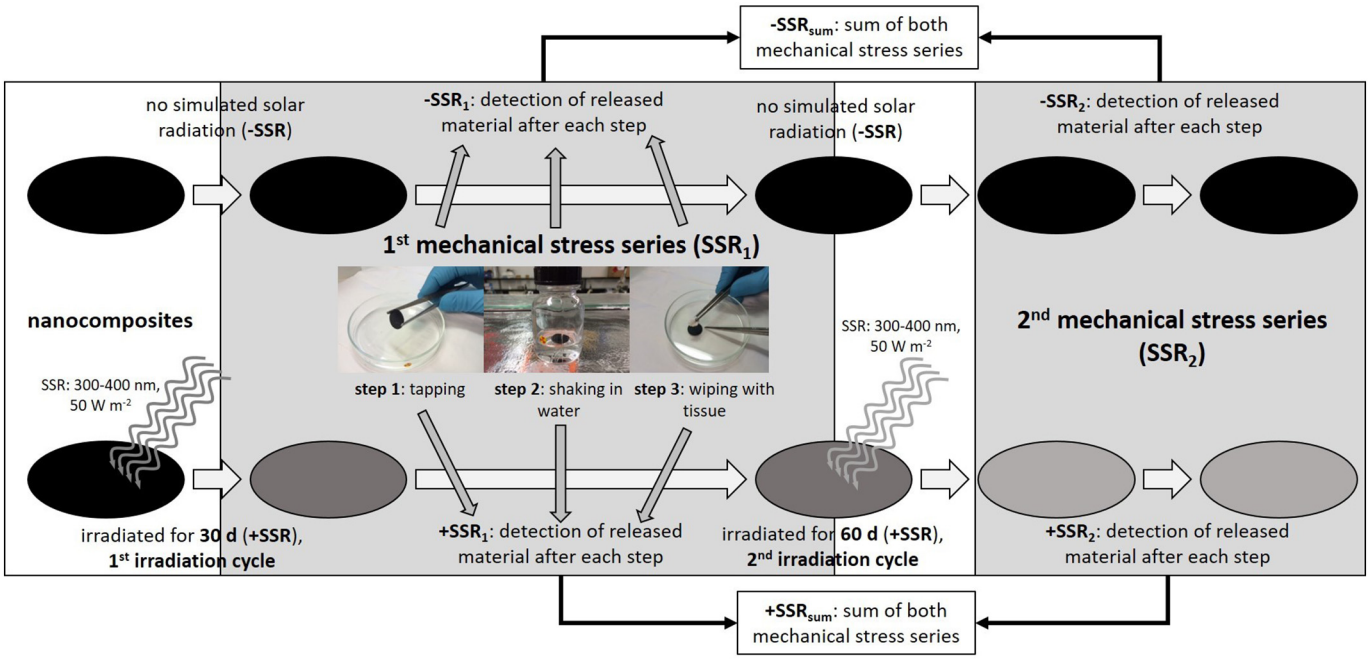

Fig. 1. Mechanical treatment experiment for determining the release of radioactivity from ^{14}C-labeled irradiated epoxy/MWCNT (E/^{14}C-MWCNT) composites (n = 4, +SSR$_1$, and +SSR$_2$) and non-irradiated E/^{14}C-MWCNT control plates (n = 2, -SSR$_1$, and -SSR$_2$). Three different mechanical treatments for the nanocomposites are depicted: the plates were tapped over a petri dish, shaken in 15 mL Milli Q water for 3 d, and finally both sides were gently wiped off once with a tissue after the first and the second irradiation cycle. The same was performed using unlabeled nanocomposites.

only one surface of the plates. The irradiance was set up at 50 W m^{-2}. Samples were placed on a water-cooled exposure table and were put in a new position once a week in order to guarantee a uniform irradiation of the composites. For the release experiments with mechanical treatment, one part of non-irradiated E-plates was exposed to two irradiation cycles: in the first cycle, one side of these plates was irradiated for 30 d (130 MJ m^{-2}). Afterwards, the first mechanical treatment series was performed for both non-irradiated (-SSR$_1$) and irradiated plates (+SSR$_1$). Composites that were initially subjected to SSR were now again irradiated for 60 d at the same surface (260 MJ m^{-2}). Then, E/MWCNT nanocomposites (-SSR$_2$ and +SSR$_2$) were treated mechanically again (Fig. 1). Non-irradiated plates (-SSR$_1$ and –SSR$_2$) served as control group for each mechanical treatment. For the release study using quartz sand-water systems, non-irradiated (-SSR) and 90 d (390 MJ m^{-2}) constantly irradiated nanocomposites (+SSR) without any mechanical treatment were used to show the influence of UV-degradation on the release of MWCNT.

2.4. Release of ^{14}C-activity by a series of mechanical treatments

Three different mechanical treatment methods were chosen for determining the release of RA from ^{14}C-labeled irradiated E/MWCNT composites (n = 4, +SSR$_1$, and +SSR$_2$) and non-irradiated radiolabeled E/MWCNT control plates (n = 2, -SSR$_1$, and -SSR$_2$) to compare the amounts of ^{14}C-MWCNT released after 30 d and 60 d of irradiation (Fig. 1).

In the first step ('tapping') the composites were carefully hold with a pair of tweezers and gently tapped ten times over a petri dish. The petri dish was then cleaned with a wet tissue, which was put in 15 mL scintillation cocktail (IRGASAFE Plus™, Perkin Elmer) and subjected to liquid scintillation counting (LSC). Afterwards, the composites were placed in 15 mL of Milli Q water ('shaking'), which was shaken for three days (160 rpm) similar to the study of Rhiem et al. (2016). The complete aqueous phase was then analyzed by LSC as well. Finally, both sides of the composites were gently wiped once with a tissue that was again subjected to LSC ('wiping'). Furthermore, unlabeled E/MWCNT and *E*-only plates were produced and irradiated as well (Fig. A2 A–B) in order to visualize their surface by scanning electron microscopy (SEM) and the released material by transmission electron microscopy (TEM). The released particles were collected in the water after shaking, concentrated by evaporation, and resolved in 0.5 mL Milli Q water for TEM measurements. Description of the SEM and TEM measurements can be found in the SI. Data are presented as the cumulative released percentage of introduced (embedded) amounts of ^{14}C-MWCNT in the composite (Table 1A) and proportions of total RA amount released during the mechanical treatment (total released RA = 100% value, Table 1B). The measured RA of the ^{14}C-labeling can be directly transformed into mass ^{14}C-MWCNT using their specific activity of (1.9 MBq/mg ^{14}C-MWCNT). The sum of released RA of all treatments and after all irradiation cycles is given as ± SSR$_{sum}$s.

2.5. Release of ^{14}C-activity in a quartz sand-water system

To study the release of RA in a quartz sand-water system, ^{14}C-labeled ± SSR E/MWCNT nanocomposites (n = 3, Fig. 2) were directly placed into glass vessels containing 8 g dry weight (dw) of pre-washed and dried quartz sand (F36, Quarzwerke Frechen, Germany) and 24 mL of reconstituted water (OECD, 1992).

In detail, at first 4 g of quartz sand was put in the glass vessel. The composites were placed on this layer and 4 g of quartz sand was added on the plate in order to cover it completely. The water was slowly and carefully pipetted along the edge of the vessel. Subsequently, vessels were closed with Parafilm® and shaken vertically at 60 rpm. Quartz sand and medium were exchanged after 1, 4, 14, 28, and 42 d. The RA in quartz sand and overlaying medium was measured for every time point using LSC. On each time point, the water phase was drained and RA was measured in the complete volume. To get the plates out of the vessels non-destructively, the upper quartz sand phase above the composite was rinsed carefully from the plate using Milli Q water. The nanocomposite was taken out carefully with tweezers and placed again serially in a new quartz sand-water system as described above. The quartz sand was dried at 104 °C for 24 h, then portioned in 1 g amounts

Table 1
A–B Released percentage of initially embedded ^{14}C-MWCNT from irradiated epoxy/^{14}C-MWCNT nanocomposites (E/^{14}C-MWCNT $n = 4$, A) based on the absolute released ^{14}C-MWCNT mass, and released proportions on each mechanical step (sum of three treatments = 100%, %, B) after different irradiation cycles (mean ± standard deviation). After the first irradiation cycle of 30 d with simulated sunlight radiation (+SSR$_1$) the plates were mechanically treated by tapping (1), shaking in water for 3 d at 150 rpm (2), and tissue wiping (3) and subsequently irradiated for another 60 d (+SSR$_2$). After the second irradiation cycle the plates were mechanically treated like after the first cycle. The relative amounts of ^{14}C-MWCNT were summed up for each mechanical treatment and irradiation scenario and the percentage of initially embedded MWCNT was determined (± SSR$_{sum}$). Sum of released material after all treatment steps is marked in bold figures. Non-irradiated composites (–SSR$_1$ and –SSR$_2$) were kept in the dark and served as controls ($n = 2$), but were treated mechanically as well. Significant differences between –SSR and +SSR were statistically examined by use of a Student *t*-test ($\alpha = 0.05$) and were marked by asterisks (*), no significance between the treatments were marked with a minus (−). The detection limit of LSC was determined as 0.21 ng ^{14}C-MWCNT (at a specific RA of 1.9 kBq µg^{-1} ^{14}C-MWCNT).

A

Treatments	1st irradiation cycle (30 d)			2nd irradiation cycle (60 d)			Σ released RA (30 + 60 d)		
	-SSR$_1$	*+SSR$_1$*	*/−	*-SSR$_2$*	*+SSR$_2$*	*/−	*-SSR$_{sum}$*	*+SSR$_{sum}$*	*/−
	Released percentage of initially embedded ^{14}C-MWCNT [%]								
Tapping (1)	0.0003 ± 0.0001	0.0016 ± 0.0005	*	0.0002 ± 0.0001	0.0003 ± 0.0002	–	0.0005 ± 0.0002	0.0019 ± 0.0004	*
Shaking (2)	0.0004 ± 0.0000	0.0074 ± 0.0035[a]	–	0.0004 ± 0.0001	0.0210 ± 0.0093	*	0.0008 ± 0.0001	0.0233 ± 0.0059[a]	*
Wiping (3)	0.0027 ± 0.0017	0.0290 ± 0.0239	–	0.0005 ± 0.0002	0.0323 ± 0.0120	*	0.0032 ± 0.0019	0.0612 ± 0.0337	–
Σ treatments	0.0034 ± 0.0018	0.0248 ± 0.0109[a]	–	0.0011 ± 0.0004	0.0536 ± 0.0195	*	0.0045 ± 0.0022	0.1046 ± 0.0664	–

B

Treatments	1st irradiation cycle (30 d)		2nd irradiation cycle (60 d)		Σ released RA (30 + 60 d)	
	-SSR$_1$	*+SSR$_1$*	*-SSR$_2$*	*+SSR$_2$*	*-SSR$_{sum}$*	*+SSR$_{sum}$*
	Proportions of total released ^{14}C-MWCNT [%]					
Tapping (1)	7.7 ± 3.9	6.5 ± 2.1[b]	12.5 ± 12.5	0.5 ± 0.3	11.4 ± 5.7	1.8 ± 0.4[b]
Shaking (2)	15.3 ± 3.5	30.0 ± 15.1[b]	37.5 ± 11.3	39.2 ± 19.0	20.0 ± 2.6	21.5 ± 6.2[b]
Wiping (3)	77.0 ± 46.2	120.3 ± 103.1[b]	50.0 ± 12.5	60.2 ± 24.7	68.6 ± 37.1	58.5 ± 34.3[b]

[a] Outlier was detected by using Dixon's Q test ($\alpha = 0.05$).
[b] Due to elimination of the outlier, the sums are not always adding up to 100%.

in scintillation vials, and RA measured by LSC (see SI). Preliminary studies showed that even after 42 d no microbial activity was measureable in quartz sand so that no $^{14}CO_2$ traps were used.

Unlabeled irradiated composites containing MWCNT and irradiated composites without MWCNT ($n = 2$) were added into a same quartz sand-water system. After 28 d both composite types were taken out and prepared for SEM and TEM analyses. An incubation period of 28 d for the unlabeled composites was chosen, because the results of the release

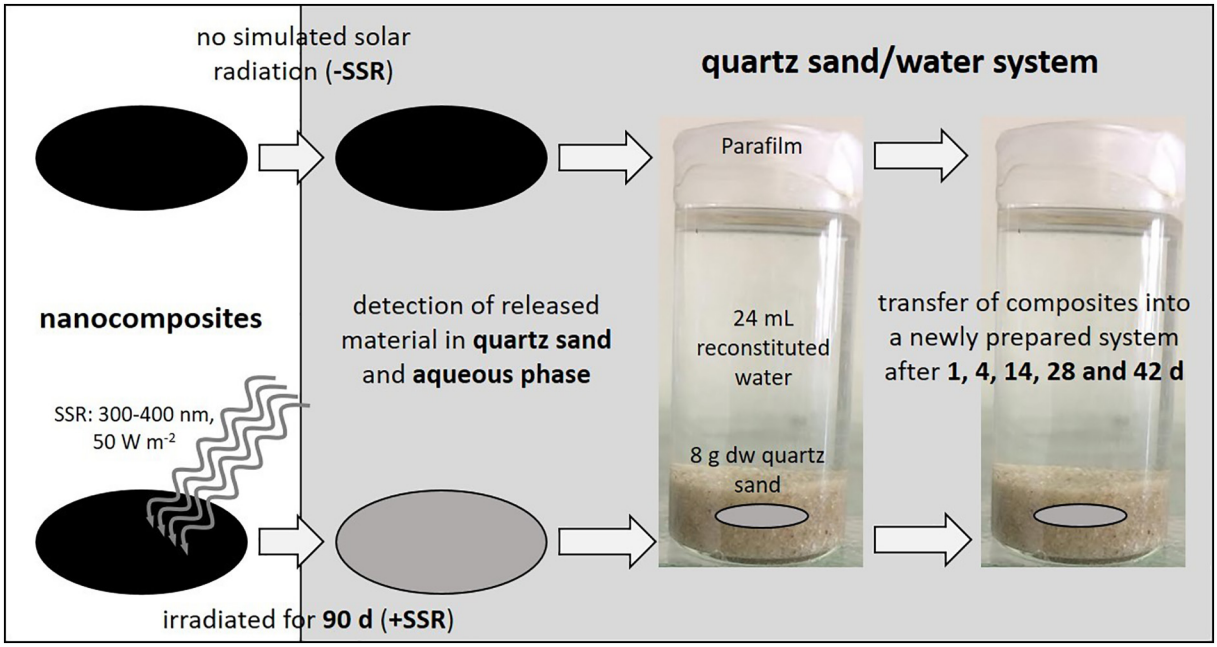

Fig. 2. Quartz sand-water system experiment for determining the release of radioactivity from ^{14}C-labeled irradiated and non-irradiated epoxy/MWCNT nanocomposites (± SSR E/^{14}C-MWCNT, $n = 3$). Plates were directly placed into glass vessels containing 8 g dry weight (dw) of pre-washed and dried quartz sand and 24 mL of reconstituted water. Quartz sand and medium were exchanged after 1, 4, 14, 28, and 42 d. The same was performed using unlabeled nanocomposites.

experiment showed that most of the RA was set free from the plates after this time. The water phase of the system was transferred to a Petri dish. The plates were taken out as described above. An amount of 15 mL Milli Q water was added to the quartz sand and the mixture slightly shaken in order to whirl up the quartz sand. As a result, the released material floated on the surface of the water phase, which could be subsequently taken out into the Petri dish. The water phase was allowed to evaporate completely until dryness at 60 °C for 24 h. The residues in the petri dish contained salts and released material and were resolved in 0.5 mL Milli Q water. This concentrated material was placed on cupper grids for TEM analyses. The surface of the plates was investigated by SEM analyses. Description of the methods using for SEM and TEM can be found in the Supporting Information (SI).

2.6. Uptake experiments with Lumbriculus variegatus

Blackworms (*Lumbriculus variegatus*) were provided from ECT Oekotoxikologie GmbH (Flörsheim, Germany) and were cultured in glass vessels (Ø 23 cm, height 8 cm) containing 2 cm washed quartz sand and 5 cm layer of aired reconstituted water. The water temperature was adjusted to 20 ± 1 °C and a photoperiod of 16 h:8 h light:dark was given. *Lumbriculus variegatus* were fed with twice a week with a stinging nettle suspension (300 mg in 10 mL MilliQ water). The water phase was changed once a week; the sediment phase was changed every five to six weeks. For the uptake experiments of released material five synchronized blackworms (OECD, 2007) were exposed for 48 h in three scenarios (Fig. 3):

A.) Released material (RM): irradiated composites (90 d, +SSR) were placed into quartz sand-water systems, which were subsequently shaken until the equilibration time was reached after 28 d for E/^{14}C-MWCNT plates (n = 3, 60 rpm). Afterwards, the organisms were introduced into the vessels.

B.) Water application (WA): amounts of 845 ng ^{14}C-MWCNT per quartz sand-water system were dispersed so that the dispersion contained the respective amount of ^{14}C-MWCNT in 24 mL of reconstituted water. This ^{14}C-MWCNT amount was chosen in respect of the maximum released RA from the plates after equilibration time during the release experiments. The volume of 24 mL dispersion was applied on 8 g dw quartz sand, already containing 2.3 mL reconstituted water (representing the maximum water holding capacity, WHC_{max} for the quartz sand). Blackworms were inserted into the vessels (n = 4).

C.) Quartz sand application (SA): the same amount of ^{14}C-MWCNT from B) were dispersed so that the dispersion contained this respective amount of ^{14}C-MWCNT in 2.3 mL reconstituted water to bring 8 g quartz sand to WHC_{max}. A volume of 24 mL reconstituted water was added on the top of the sand without mixing and the organisms were introduced into the vessels immediately afterwards (n = 4).

For B) and C) 26 and 28 µg of ^{14}C-MWCNT was weighted at a microbalance (MYA 5.3Y, Radwag) and added into 330 and 40 mL of aqueous medium, respectively. The MWCNT were dispersed by using an ultrasonic disintegrator with a microtip twice for 10 min (Sonopuls HD 2070, 70 W, pulse: 0.2 s, pause: 0.8 s). Rhiem et al. (2015) showed that this method is appropriate for dispersing MWCNT in aqueous solutions since only small agglomerates and single MWCNT (0.2 to 1.0 µm) were detected using TEM. The RA in the dispersions was measured before the exposure in order to control the initial conditions. Control vessels (n = 4) with the same scenarios as described above were set up, just only with unlabeled MWCNT and +SSR nanocomposites. Additionally, a control scenario only with quartz (n = 4) sand was prepared in the same way. No mortality of blackworm was detected in all control treatments after 2 d of incubation.

After the exposure time, the organisms were taken out of the vessels and cleaned once with reconstituted water in order to detach associated RA from the surface of the worms. RA in 10 mL water containing worm faeces was quantified by LSC. After 24 h worms were taken out of the vials and homogenized in a small glass mortar and 0.5 mL methanol

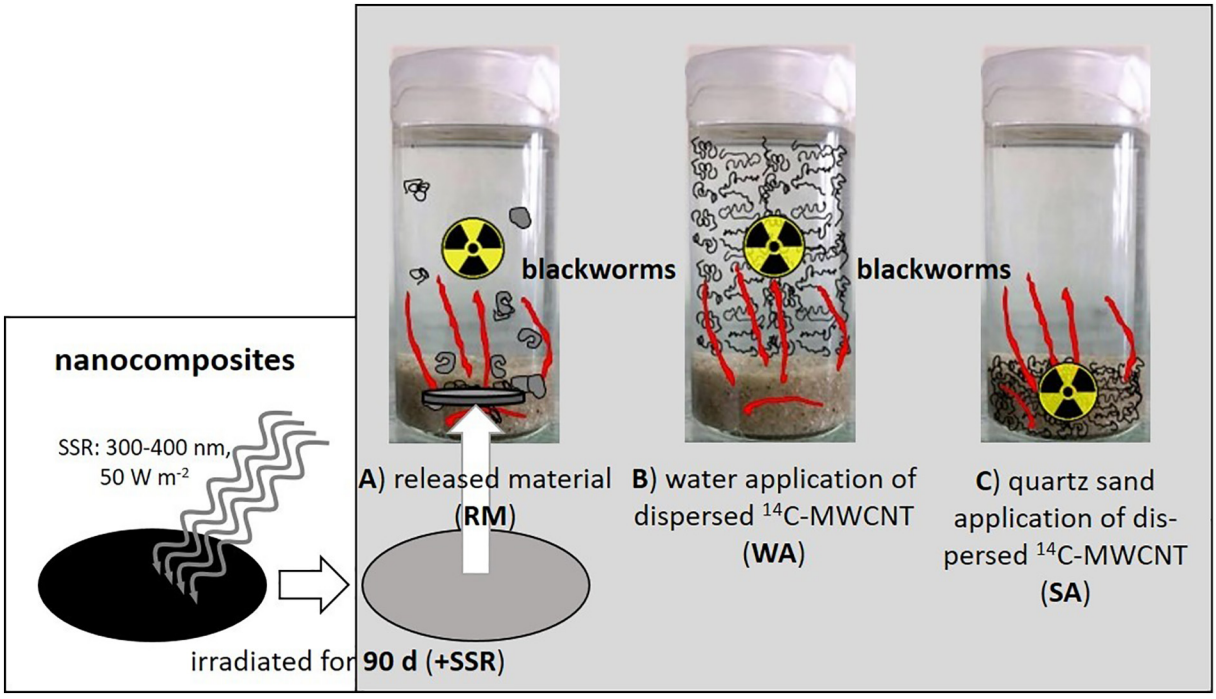

Fig. 3. Uptake experiments of radioactivity (RA) in three different scenarios: Five blackworms were exposed to A) released material from ^{14}C-labeled irradiated epoxy/MWCNT composites (+SSR E/^{14}C-MWCNT, RM, n = 3), B) ^{14}C-MWCNT applied to the water phase of the quartz sand-water system (WA, n = 4) and C) ^{14}C-MWCNT applied to the quartz sand before adding water to the system (SA, n = 4) for 2 d. After uptake of RA, excretion was observed for 24 h by transferring the worms to reconstituted water.

(≥99.9%). This homogenate was transferred into a scintillation vial and measured by LSC. The RA in the water phase, quartz sand phase, and excretes were determined by LSC. The values for 'worm and faeces' are the sum of 'faeces' and 'worm after elimination' (Fig. 7). The biota sediment accumulation factor (BSAF) was determined in all three scenarios (Ankley et al., 1992).

2.7. Data evaluation

Data were processed by using Microsoft Excel® (Microsoft Office Professional Plus 2016), GraphPad Prism (GraphPad Prism 6, USA), and SigmaPlot (SigmaPlot Version 12.0, USA). All data was tested for outliers using the Dixon's Q test ($\alpha = 0.05$). Differences between treatments (-SSR and +SSR) after mechanical treatment and in quartz sand-water system were examined by use of a Student *t*-test ($\alpha = 0.05$). Furthermore, for significant differences between the application scenarios RM, WA and SA a multivariate ANOVA was performed (function manova in R, R Core team, 2017). For the comparison of the BSAF between these scenarios, a One Way ANOVA was performed ($\alpha = 0.05$). Data were checked for normality distribution with Shapiro-Wilk's test (function shapiro.test in R) and for variance homogeneity with Levene's test (function leveneTest in R).

2.8. Acronyms

In this section, the most important acronyms used in this text were explained.

SSR simulated sunlight radiation

+SSR irradiated with simulated sunlight

–SSR non-irradiated control group

RM 'released material' – blackworm was exposed to released E/MWCNT fragments

WA 'water phase application' – blackworm was exposed to dispersed MWCNT from water phase

SA 'quartz sand application' – blackworm was exposed to dispersed MWCNT from quartz sand

3. Results

3.1. Surface alteration and MWCNT release after weathering and mechanical treatment of E/MWCNT

3.1.1. Electron microscopy of E/MWCNT surfaces and released material

Comparing the surface areas of E/MWCNT plates of all treatments, plates being non-irradiated showed a very homogenous, smooth, and plain surface (Fig. 4A). Only few and slight indentations as well as protrusions were visible. In contrast, SSR and mechanical treatment appeared to alter the plate surfaces (Fig. 4B–D, black arrows). The surface of samples irradiated for one month showed formation of small round-shaped structures (with a diameter of max. 5 µm) over the entire area (Fig. 4B). After three months of irradiation without any mechanical treatment, a further decomposition of the epoxy polymer on the surface was observed, resulting in clearly visible structures protruding from the surface (Fig. 4C). These structures were similar to the pattern observed in Fig. 4B, but more pronounced. In Fig. 4D, additional lesions on the composite surface are visible.

The TEM results revealed that released particles consisted of epoxy polymer with embedded and partially free MWCNT agglomerates and also single string MWCNT protruding from the edge of the fragments (Fig. 4D–F, white arrows). Released polymer fragments from the epoxy composites itself, i.e., without embedded MWCNT, after three months of irradiation were also detected having similar structures (see Fig. 4E–G and Fig. A3 B, C). Regarding the composites, the agglomerates were mostly still embedded in the epoxy polymer matrix (Fig. 4D). The diameter of the released material was estimated in the nm range (Fig. 4E, F). Protruding MWCNT fibres were visible and had a length of about 200 nm when measuring from the edge of the epoxy polymer fragment.

3.1.2. Quantification of ^{14}C-MWCNT

After all mechanical treatments and irradiation cycles 0.10 ± 0.07% of the initially embedded RA in the composites was released (Table 1A). From the non-irradiated control group 0.0045 ± 0.0022% of the initially embedded RA was set free. The intensity of mechanical stress increased over the three treatment steps that both the weathered and non-irradiated were serially exposed to (Table 1B). This resulted in a gradual enhancement of release of MWCNT material during the complete conducted sequence.

After the first irradiation cycle and the mechanical step (tapping) only a ca. 5- fold higher release of ^{14}C-labeled MWCNT from the plates was measured than for non-irradiated samples (Table 1A). After the second irradiation cycle and subsequent 'shaking' and 'wiping', this significant difference was greater by a factor of 53 and 65. Hence, release of RA from +SSR plates after the second irradiation cycle during all three mechanical steps was significantly higher (about 50 times) than for $-SSR_2$ plates. Regarding the summed up release for each mechanical treatment step, the sum of released material after both 'tapping' and 'shaking' steps was significantly higher for $+SSR_{sum}$ plates than for $-SSR_{sum}$ composites (3.8- and 29-fold). After all irradiation cycles and mechanical procedures an amount of about 0.93 ± 0.59 µg ^{14}C-MWCNT have been released from $+SSR_{sum}$ plates and 0.035 ± 0.015 µg ^{14}C-MWCNT from the control group ($-SSR_{sum}$). Due to high scattering of the data, the significance of this difference could not be indicated.

Mass release after the first or second treatment series only (as the sum of all three treatment steps after the first or second irradiation, in ng) and total mass release after both treatment sequences (as the sum of mass release after the first and second treatment series) were divided by the surface area of the plate (in cm^2). Calculating with a plate diameter of 18.2 mm (surface of about 5.2 cm^2), approximately 0.050, 0.015, and 0.067 mg MWCNT m^{-2} were released from the non-irradiated samples after the first and the second treatment series only and in sum after both complete mechanical procedures, respectively. For +SSR plates it has to be considered that only one side of the composite was irradiated so that only 2.6 cm^2 were subjected to SSR. In order to determine the correct released amount caused by SSR only, the released low amount from the control plates has to be subtracted from the released amount of the +SSR plates. This resulted in a released absolute amount of about 0.723, 1.776, and 3.421 mg MWCNT m^{-2} by SSR only, after the first and the second irradiation cycle and after the complete mechanical treatment sequence, respectively.

3.2. Release in quartz sand-water systems

3.2.1. Electron microscopy of E/MWCNT surfaces and released material

The incubation of the composite in quartz sand led to significant alterations of the surface, comparing the surface of one and three month irradiated plates that were not placed in a quartz sand-water system afterwards (Fig. 4C and Fig. 5A). All over the surface of the plate, round- and fiber-shaped protruding structures were observed (Fig. 5A, black arrows).

Regarding the released material polymer fragments containing filamentous structures as well as single strings and protruding fibres from epoxy polymer were observed (Fig. 5B, C, white arrows). These structures indicated the presence of released MWCNT, since a comparison of released material from epoxy composites without embedded MWCNT (Fig. A3 B, C) and MWCNT containing plates (Fig. 5B) showed that the shape of the released polymer fragments were similar, except the fiber structures. The released fibres had a similar diameter (about 20 nm) as the used MWCNT Baytubes®. In Fig. 5C MWCNT were found as free strings, but were shorter with lengths of 200–500 nm than that classified by the producer (length of several µm). This possible destruction

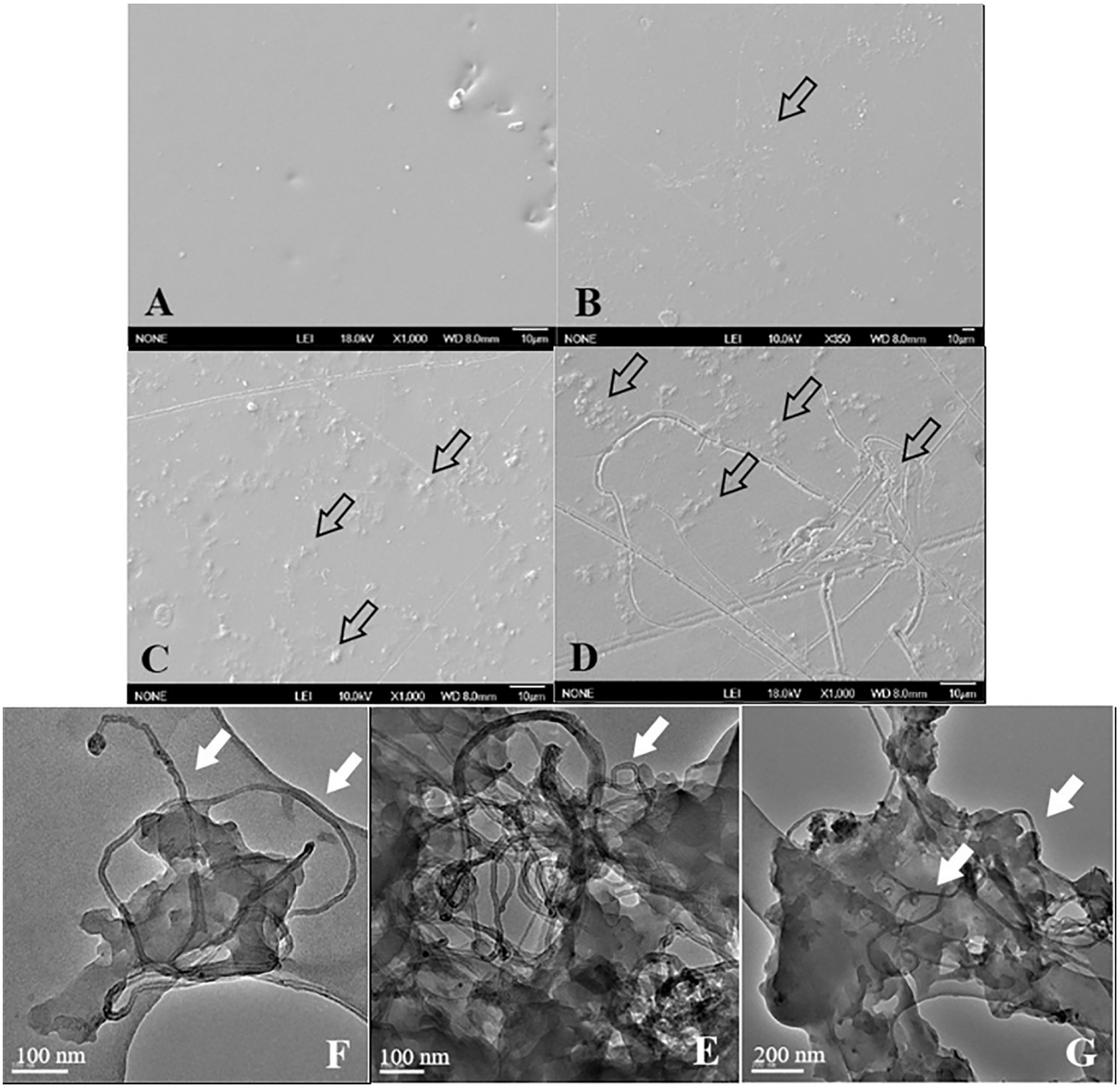

Fig. 4. A–G Scanning electron microscopy (SEM) images from the surface of non-irradiated epoxy/MWCNT (E/MWCNT) plates (A) and plates irradiated for 30 d (B) and 60 d (C). Fig. D shows the composite surface after 30 d irradiation and the first mechanical treatment series (tapping, shaking in water, and gentle wiping). Transmission electron microscopy (TEM) images were obtained from released E/MWCNT fragments (D–F) and show protruding MWCNT from the polymer fragments (E). This material was released during the water shaking process after the second irradiation cycle of 60 d. Black and white arrows highlight the most important found structures.

may be caused by the long ultrasonication time of the MWCNT using a microtip.

3.2.2. Quantification of ^{14}C-MWCNT

The cumulative released percentages of initially embedded RA per E/^{14}C-MWCNT composite was always significantly higher (ca. 23-fold) for +SSR plates than for -SSR composites ($\alpha = 0.05$) in quartz sand (Fig. 6). The corresponding cumulative absolute amount of released ^{14}C-MWCNT into quartz sand were 0.033 ± 0.005 μg and 0.838 ± 0.228 μg for non-irradiated and irradiated *E*-plates (data not shown). It must be considered that $8.0 \times 10^{-4} \pm 1.9 \times 10^{-4}$% of embedded RA (7.3 ± 1.8 ng) was released from +SSR nanocomposites into the water phase after 42 d (Fig. 6, triangles), resulting in a cumulative released amount into the complete system (solid and aqueous phase) of 0.845 ± 0.230 μg ^{14}C-MWCNT and 0.0914 ± 0.0215% of initially embedded ^{14}C-MWCNT. This means that 99.1 ± 27.0% of total released RA was found in quartz sand and only 0.9 ± 0.2% in the water phase. This was expected since the plates were placed into the solid phase at the beginning of the experiment.

With an average diameter of 18.2 mm for the E-plates, about 0.063 mg MWCNT m^{-2} and 3.123 mg MWCNT m^{-2} were set free from non-irradiated and irradiated composites into the complete quartz sand-water system after 42 d, respectively, indicating a 49-fold stronger release of ^{14}C-MWCNT into the system due to SSR treatment, based on the surface normalized values. It is important to mention, that cumulative released % of RA is based on the mass of MWCNT, which are initially embedded in the nanocomposites, whereas surface normalized values are based on the (weathered) composite surface from which MWCNT can be released. The higher factor of 49 using the surface normalized values comes from the fact, that only one side of the plates was subjected to SSR, which roughly doubles the factor calculated from the MWCNT mass in the composite. Furthermore, for the +SSR plates over 93% of the released RA to the quartz sand fraction was already set free after day 4, whereas only 69% of released RA to the sand phase was

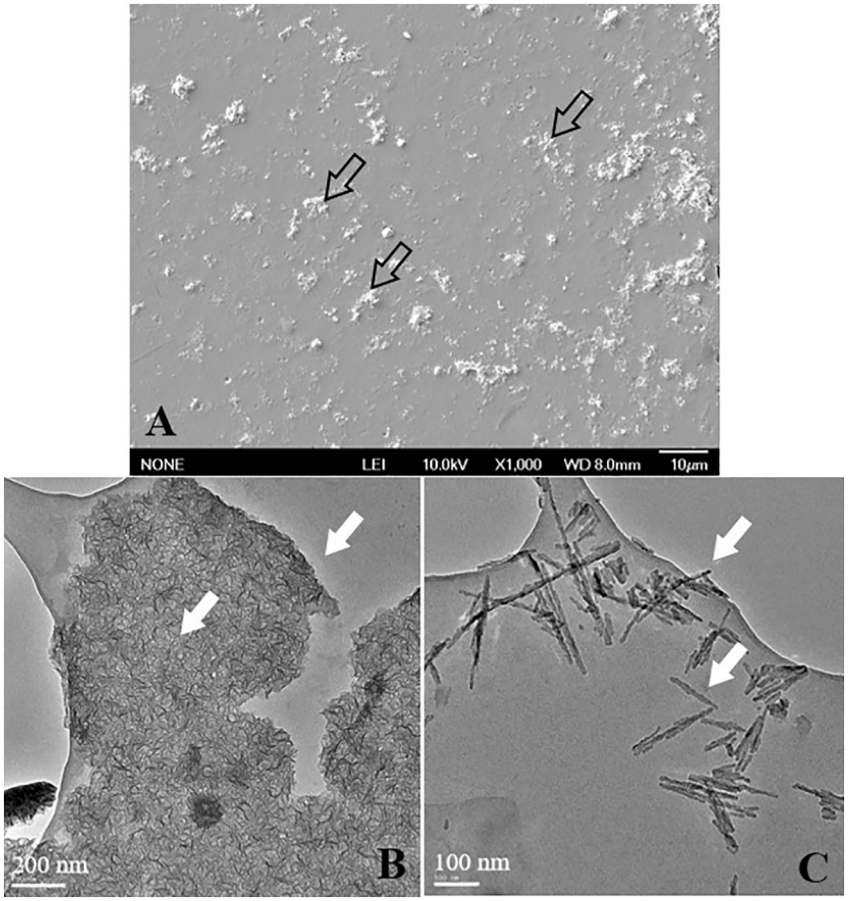

Fig. 5. A–C Scanning electron microscopy (SEM) images from the surface of an irradiated epoxy/MWCNT (E/MWCNT) plate (A) after shaking in quartz sand for 28 d. The fragments (B–C) were analyzed by transmission electron microscopy (TEM). Black and white arrows highlight the most important found structures.

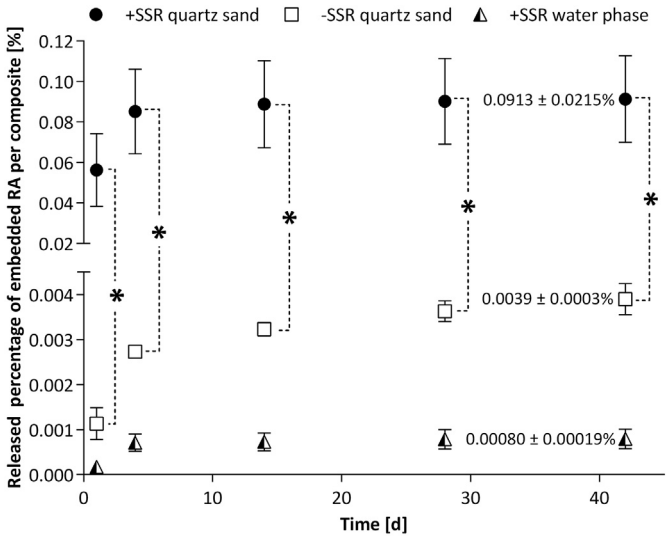

Fig. 6. Released radioactivity (RA) from irradiated epoxy/^{14}C-MWCNT (+SSR E/^{14}C-MWCNT) composites into quartz sand (filled dots) and water phase (half-filled triangles). Non-irradiated plates (-SSR) as control group for quartz sand release (open squares). All data are presented in percent of the initially embedded RA per composite (%, $n = 3$) after 42 d and as mean ± standard deviation (whiskers). All quartz sand data points for +SSR E/^{14}C-MWCNT plates are significantly higher than data points of –SSR composites ($\alpha = 0.05$). Analysis of RA from +SSR plates into water phase was near the detection limit. However, for –SSR treatment the amount of RA lied below the detection limit (< 0.21 ng ^{14}C-MWCNT).

released from –SSR plates at the same time point. All measured values for RA in the water phase from –SSR plates were below the detection limit (0.21 ng ^{14}C-MWCNT).

3.3. Uptake of released material by Lumbriculus variegatus

Multivariate ANOVA revealed a significant difference of the three independent scenarios (RM, WA, SA) on the dependent compartments (water, sand, faeces, worm after elimination) with a *p*-value of 0.011 (Fig. 7). For RM the complete released amount of ^{14}C-MWCNT in the quartz sand-water system amounted to 0.37 ± 0.27 µg, corresponding to initially embedded RA of 0.038 ± 0.026% (data not shown). These release values were about 43% lower compared to release experiments into quartz sand-water systems (0.85 ± 0.23 µg ^{14}C-MWCNT). About 2.5 ± 1.2% of released amount of ^{14}C-MWCNT were found in the aqueous phase, corresponding to 9.3 ± 4.4 ng ^{14}C-MWCNT. The RA was mainly found in quartz sand phase with about 93 ± 1% (RM), 70 ± 3% (WA), and 75 ± 2% (SA). The recoveries of the initially applied RA in WA and SA were 90 and 95%. For RM, no recovery could be given, since the released RA from the nanocomposite was set up to 100%.

It was found that 66% of the material ingested by the black worms in the RM scenario was eliminated again after 24 h, whereas it was 96% and 75% for the WA and SA scenarios (Fig. 7). For all three scenarios a biota-sediment accumulation factor (BSAF) could be estimated, only considering the amounts of RA in the quartz sand phase. In the RM scenario a BSAF of 0.020 ± 0.010 was calculated, whereas it was 0.003 ± 0.001 and 0.020 ± 0.018 for WA and SA, respectively. These BSAF were not significantly different from each other and thus all scenarios indicated low bioaccumulation of released E/^{14}C-MWCNT

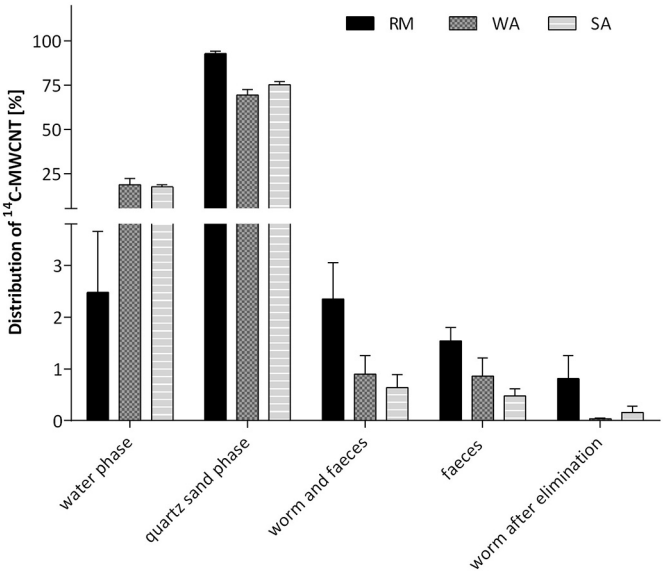

Fig. 7. Distribution of radiolabeled MWCNT (^{14}C-MWCNT) in the quartz sand-water system and uptake/elimination of RA by blackworm in three different scenarios: released material fragments from irradiated epoxy/^{14}C-MWCNT composites (RM, $n = 3$), water phase application of ^{14}C-MWCNT (WA, $n = 4$) and quartz sand application of ^{14}C-MWCNT (SA, $n = 4$). In each scenario the blackworm *Lumbriculus variegatus* was added for uptake experiments of RA. The amount of ^{14}C-MWCNT was chosen with respect to the released RA from the release experiments. Statistical analysis by a multivariate ANOVA showed a significant difference of the three independent scenarios (RM, WA, SA) on the dependent compartments (water, sand, faeces, worm after elimination) with a p-value of $0.011 < 0.05$.

fragments and ^{14}C-MWCNT.

4. Discussion

4.1. UV-degradation of E/MWCNT composite surfaces

The gradual uncovering of MWCNT agglomerate structures after irradiation with SSR protruding from the surface of the nanocomposite seem to be still covered by a layer of epoxy polymer (Fig. 4A–C), indicating that the exposed irradiation dose does not cause a complete decomposition of the uppermost epoxy layer. Thus, no free MWCNT network was detected on the surface. Irradiation in this study corresponds to natural sunlight irradiation periods of 4.3, 8.7, and in sum, 13.0 months, respectively, in Europe at 50° northern latitude (Wohlleben et al., 2011a; Hirth et al., 2013). Many studies present UV-degradation of different polymer materials, in which MWCNT were incorporated, like polycarbonates, polyurethanes, epoxy resins, or polyamides (Vilar et al., 2013; Rhiem et al., 2016; Wohlleben et al., 2016; Koivisto et al., 2017; Neubauer et al., 2017; Nguyen et al., 2017). Especially for E/MWCNT nanocomposites, several studies exist that show a fast photo-degradation of the epoxy polymer and a formation of a MWCNT network on the surface (Nguyen et al., 2009; Ging et al., 2014; Kingston et al., 2014; Petersen et al., 2014). Nguyen et al. (2017) reported rapid photo-degradation (295–400 nm) of amine-cured epoxy resin in E/MWCNT (0.72% w/w) surfaces, which were additionally exposed to a relative humidity of 75% at a temperature of 50 °C. Comparing SEM pictures from the abovementioned studies, a similar degradation pattern of epoxy resin on the surface in our study is observable, presenting a slow but gradual uncovering of MWCNT networks on the surface of the nanocomposite from low to high exposure times. These networks concentrate and agglomerate on the exposed composite surface. The epoxy decomposition by simulated sunlight in this study is obviously not far proceeded, since mainly covered MWCNT agglomerates with a thin layer of epoxy resin were still visible, in contrast to studies of Nguyen et al. (2017). It must be considered that the irradiation intensities were different in that study and that the additional weathering processes (humidity) may significantly enhance epoxy degradation.

Comparing all UV-degradation studies with E/MWCNT nanocomposites, protruding MWCNT amounts on the composite surfaces were independent from MWCNT loadings in the composites (Schlagenhauf et al., 2015b). Schlagenhauf et al. (2015b) presented similar results for surfaces of E/MWCNT (1% w/w), which were subjected to UV-light (340 nm, 0.89 W/m^2) for at most two months with a relative humidity of < 5%. Smooth and rough 'islands' have been observed on the exposed surface, indicating low and high UV-exposed areas. Further microscopic images confirmed that the surface layer above the smooth 'islands' was delaminated and that a loss of matrix occurred. This resulted in fast deceleration of the epoxy surface degradation by agglomeration of the much more UV-resistant MWCNT network that finally remained on the composite surface forming a UV-protecting layer (Nguyen et al., 2017).

4.2. Qualitative analysis of E/MWCNT composites after mechanical treatment and within a quartz sand-water system

The TEM images of released E/MWCNT material after mechanical treatment (Figs. 4 and 5) revealed loose polymer fragments in the range of several hundred nm to µm, containing MWCNT structures and free MWCNT fibres protruding from the polymer matrix. It was clearly visible that mechanical treatment and shaking in the quartz sand-water system led to further decomposition of the epoxy layer of irradiated E/MWCNT (Figs. 4D and 5A), as brighter spots and further protruding MWCNT network appeared. However, even a second irradiation cycle and a subsequent second treatment series did not remove the covering epoxy layer on the surface. The surrounding polymer of the visualized MWCNT structures appeared to be stable enough to hinder free release of MWCNT (Fig. 4B, C). However, TEM results (Fig. 4E–G and Fig. 5B, C) revealed that the UV-degraded epoxy top layer fragments seem to delaminate from the exposed surface that contained a MWCNT network as well as single MWCNT. The presence of water within the system and the presence of tiny cracks in the surface of the plate, caused by UV-irradiation, enhanced this peeling-off process. Furthermore, ions in the aqueous phase would have an influence on the peel-off effect, depending on their concentration and their type. In their presence, water chemistry can be altered, especially in terms of pH or ionic strength. Some ions can cause strong pH variations, which might destabilize the already brittle and oxidized epoxy polymer surface and MWCNT. This could enhance the breaking off of already loosely attached fragments and hence lead to a stronger release. Quantitative results by Rhiem et al. (2016) support this explanations. Higher aqueous ionic strength could lead also to a re-arrangement of the uncovered MWCNT on the composite surface. Systematic research on the influence of water chemistry on polymer degradation is lacking.

These results are widely consistent with observations in many other studies that examined the release of irradiated polymer/MWCNT nanocomposites after abrasion, sanding, and eventual weathering (Cena and Peters, 2011; Hirth et al., 2013; Schlagenhauf et al., 2015a; Schlagenhauf et al., 2015b; Neubauer et al., 2017; Wohlleben et al., 2017). Gojny et al. (2005) suggested four possible fracture mechanisms after mechanical treatment of E/MWCNT composites: (i) MWCNT can be pulled out from the matrix due to weak interfacial adhesion, (ii) ruptured from the surface through strong interfacial adhesion, (iii) pulled out telescopically by stronger interfacial bonding than Van der Waals forces between the tube layers, (iv) or finally can detach partially from the interface via the formation of crack bridges. Hence, it seems that the release of MWCNT material observed in the present study can be compared to the release presented in sanding abrasion studies.

4.3. Quantification of MWCNT from E/MWCNT after mechanical treatment and within a quartz sand-water system

Manual mechanical treatment and treatment in a quartz sand-water system after irradiation led to an increased release of loose and photo-degraded matrix particles containing MWCNT with comparable amounts (Table 1 and Fig. 6). Similar to the study of Rhiem et al. (2016), 'water shaking' led to further release of polymer fragments containing ^{14}C-MWCNT that were originally connected to the surface matrix or to a free MWCNT network (Table 1A). The same phenomenon seemed to have occurred in the test, in which the test plates were put in a quartz sand-water system. It was assumed that sand particles slowly abrade the attached loose fragments. The UV-irradiated surface layer, which basically consisted of a MWCNT network with brittle epoxy fragments containing MWCNT, was rapidly scratched off by the quartz sand particles within a short time period. Released fragments were mainly found back in the quartz sand, because the epoxy resin plates were deliberately placed in the quartz sand at the beginning of the experiment. Only a very small amount of RA was suspended in the water phase. The energy for the abrasion of these loosely attached epoxy fragments by quartz sand particles is mainly given by the slight but constant movement of the systems (60 rpm); under station conditions the released amount is expected to be much lower, since the direct interaction between the sand particles and the weathered composite surfaces is weaker. Furthermore, the density of epoxy resin is higher than that of water (1.2 g cm^{-3}), resulting in a stay on the bottom of the systems.

Wohlleben et al. (2013) suggest that moisture might be a significant *co*-factor for a faster UV-decomposition of polymers. Rhiem et al. (2016) applied similar mechanical stress to irradiated (1000 MJ/m^2) polycarbonate/^{14}C-MWCNT composites and found that the released fraction amounted to 1.1 ± 0.1% of initially embedded ^{14}C-MWCNT. Hence, release rates were higher but still in the same range as in the present study. Furthermore, similar MWCNT amounts as found by Rhiem et al. (2016) were detected after sample tapping (0.0010 ± 0.0011% of embedded ^{14}C-MWCNT), but more material was observed to be released after water shaking for 21 d (0.19 ± 0.12% of embedded ^{14}C-MWCNT) followed by tissue wiping (0.30 ± 0.11% of embedded ^{14}C-MWCNT). It must be mentioned that Rhiem et al. (2016) produced polycarbonate nanocomposites with a higher loading of MWCNT (1% w/w) and subjected the plates to a higher irradiation dose. Studies revealed, that the rapid epoxy polymer degradation led to an uncovering of the free MWCNT network, which caused the epoxy layer below to be shielded against further photo-degradation (Hirth et al., 2013; Rhiem et al., 2016; Wohlleben et al., 2017).

A total amount of 3 mg MWCNT m^{-2} was set free from +SSR plates after applying both manual and environmental mechanical stressors. Assuming that UV-radiation (300–400 nm) was the main factor for epoxy decomposition on the composite surface and considering a yearly sunlight dose in the wavelength range 300–400 nm of 360 MJ m^{-2} year^{-1} in Europe (Hirth et al., 2013), our determined release rate would correspond to about 3 mg MWCNT m^{-2} year^{-1}. This result corresponds to determined slightly higher release rates in other studies (Wohlleben et al., 2011a; Hirth et al., 2013; Rhiem et al., 2016). The difference might depend on the degradation behaviour of the various used polymer materials, the MWCNT loading, and experimental conditions such as irradiation under dry vs. humid conditions.

4.4. Bioaccumulation of released material in aquatic organisms

Recalculating the release rates obtained from the results of the present study, concentrations of 300 ng ^{14}C-MWCNT L^{-1} in the water phase (Fig. 6) and 105 µg ^{14}C-MWCNT kg^{-1} in the quartz sand compartment (Fig. 6) were found. In several studies environmental concentrations of MWCNT were predicted in surface waters and sediments by a probabilistic material-flow model and were estimated in the ng L^{-1} and the µg kg^{-1} range, respectively (Gottschalk et al., 2013a; Sun et al., 2014; Sun et al., 2016). For example, Sun et al. (2016) calculated a predicted concentration of 0.97 ng MWCNT L^{-1} in surface waters and 19.7 µg MWCNT kg^{-1} for the distribution to sediments for 2020. Hence, comparable but higher values are presented here after application of drastic mechanical stress to MWCNT composites.

Disposal of plastic debris attracted a high level of public attention during the last decades (Derraik, 2002; Thompson et al., 2009). In 2010, 275 megatons of land-borne plastic waste were produced, of which about 13 megatons are expected to end up in fresh water, oceans, and seas (Lechner et al., 2014; Jambeck et al., 2015; Ivleva et al., 2017). Degradation processes by photolysis, thermal energy and microbial activity, or mechanical decomposition by abrasion in sediments or soils are expected to lead to the formation of tiny plastic fragments, so-called micro- (< 5 mm) and nano- (< 1 µm) plastics (Thompson et al., 2004; Barnes et al., 2009; Andrady, 2011; Gigault et al., 2018). The released material from E/MWCNT nanocomposites in this study share a similar environmental fate as such plastic fragments.

Considering the transfer of E/MWCNT fragments from quartz sand into the aqueous phase, about 9 ng MWCNT were found in the presence of blackworms (*Lumbriculus variegatus*) compared to the study without blackworms (about 7 ng, Figs. 6 and 7), probably due to bioturbation of the blackworms causing a whirling up of released material when searching for food. Irradiated E/MWCNT plates in the RM-scenario were placed in the quartz sand phase at the beginning of the experiment and were not mechanically disturbed by taking them out, whereas in the release study the plates were carefully transferred into new vessels at each sampling time. These disturbances may have caused an additional scratching of the plates and this might be the reason why about twice the amount of RA was set free in the bioaccumulation study compared to the release studies without blackworm (840 ng vs. 370 ng MWCNT). However, an environmental realistic scenario for the main release process by solid particle abrasion from nanocomposites and uptake of this material could be investigated in this study.

Although all three scenarios (RM, WA, SA) were shown to be significantly different to each other, the RA distribution, between quartz sand, water, worm and faeces was similar (Fig. 7), especially for WA and SA. This can be explained by the low dispersibility and dispersion stability of MWCNT in aqueous media. Once MWCNT are dispersed in an aqueous phase, they rapidly form aggregates due to their hydrophobic nature (Glomstad et al., 2018). This agglomeration behaviour subsequently leads to a rapid deposition of MWCNT on the bottom of a water body. Several studies report about limited mobility of CNT in aquatic systems after agglomeration, leading to a ultimate deposition of the material in sediments that serve as a long-term sink (Gottschalk et al., 2013b; Schierz et al., 2014; Sun et al., 2016).

In all three scenarios studied, most of the incorporated material after uptake was excreted by the blackworms within 24 h, and hence, very low BSAF of at most 0.020 ± 0.018 were obtained in each case. These results correspond to those of other studies in which the uptake of MWCNT and micro- or nanoplastics by several aquatic and terrestrial organisms were examined. Petersen et al. (2008b) found low BSAF for SWCNT and MWCNT artificially spiked to sediments, amounting to 0.28 ± 0.03 and 0.40 ± 0.10 after 28 days of exposure of *Lumbriculus variegatus*, respectively. Low bioaccumulation factors (BAF) for SWCNT and MWCNT were also determined for many other aquatic and terrestrial organisms like algae, planktonic crustacea, oligochaetes, and fish (Petersen et al., 2008b, a; Petersen et al., 2009; Maes et al., 2014; Rhiem et al., 2015). Consequently, little or no absorption of these materials from the gut tract to other tissues is expected (Bjorkland et al., 2017).

As sediments act as sinks for high-density micro- and nanoplastics, benthic organisms are exposed to a larger extent than pelagic organisms. Redondo-Hasselerharm et al. (2018) figured out that the sediment-dwelling blackworm *Lumbriculus variegatus* is able to ingest

polystyrene microplastic particles (20–500 µm) from sediment; corresponding results were obtained by others (Wright et al., 2013; Chua et al., 2014; Setala et al., 2014; Rhiem et al., 2015). This could also be confirmed in the present study, in which uptake and depuration of epoxy polymer fragments containing radiolabeled MWCNT by the blackworm was shown.

Ingested microplastic particles might be trophically transferred to primary producers and finally reach secondary consumers in marine and freshwater systems (Farrell and Nelson, 2013; Setala et al., 2014; Watts et al., 2014; Batel et al., 2016). For example, Cedervall et al. (2012) showed that 25 nm nano-polystyrene particles were transferred through an aquatic food chain consisting of *Desmodesmus* sp., *Daphnia magna*, and *Carassius carassius*, which influenced the lipid metabolism and behaviour of the fish. However, so far no bioaccumulation into lipid tissues or biomagnification of microplastics was observed (Duis and Coors, 2016). Several publications present adverse sublethal effects on aquatic organisms caused by micro- and nanoplastics, like algae, crustacea, annelida, or fish (Casado et al., 2013; Rochman et al., 2013; Wright et al., 2013; Rochman et al., 2014; Besseling et al., 2017a; Hurley et al., 2017). These effects seem to occur mainly due to ingestion of microplastics resulting in reduced uptake of food, which might then lead to the lower availability of energy reserves causing associated effects on physiological functions.

Also acute toxic effects of MWCNT for aquatic organisms were reported (Schwab et al., 2011; da Rocha et al., 2013; Cimbaluk et al., 2018). Oxidative stress, membrane disruption, and genotoxicity due to DNA damage can be counted to the main toxicity mechanisms associated with MWCNT (Farre et al., 2009). All effects caused by MWCNT and micro- and nanoplastic occurred at concentrations in the mg L^{-1} or g kg^{-1} range, which is about six orders of magnitude higher than the predicted environmental concentrations in surface waters (ng L^{-1}) and sediments (µg kg^{-1}) (Gottschalk et al., 2013b; Jackson et al., 2013; Koelmans et al., 2015). Taking these facts into consideration it appears to be important to perform more research with long-term exposure using different endpoints at environmentally relevant concentrations of such materials.

5. Conclusion

We showed that micro- and nano-sized plastic material containing MWCNT released under realistic environmental conditions was ingested and egested by the blackworm *Lumbriculus variegatus*. More than 2000 tons of MWCNT per year are expected be synthesized in the future. Considering the amount of applications of MWCNT nanocomposites, approximately 90% (1800 tons) of the produced MWCNT are then embedded as nanofillers in plastic products and will probably be disposed after use. Calculating with the produced amount of plastic products of in 2010 (275 megatons), a proportion of only 0.0007% would belong to MWCNT nanocomposite products produced in one year. Although the amount is low compared to other bulk products, further studies for a proper environmental risk assessment of such materials in view of increasing production rates of MWCNT and plastic products is definitely necessary.

Acknowledgements

We thank the members of the project Sustainable Nanotechnologies (SUN) that receives funding from the European Commission Seventh Framework Programme (FP7/20072013) under grant agreement n° 604305 (www.sun-fp7.eu). Our special thanks go to Dr. Julie Muller and Dr. Nadir Kchit from the company Nanocyl for their support concerning the establishment of a standard operation procedure of E/^{14}C-MWCNT nanocomposites. Furthermore, we want to thank Dr. Oliver Schlüter (Bayer Technology Services) for the synthesis of ^{14}C-labeled MWCNT.

Appendix A. Supplementary data

Supplementary data to this article can be found online at https://doi.org/10.1016/j.impact.2019.100159.

References

Andrady, A.L., 2011. Microplastics in the marine environment. Mar. Pollut. Bull. 62, 1596–1605.
Ankley, G.T., Cook, P.M., Carlson, A.R., Call, D.J., Swenson, J.A., Corcoran, H.F., Hoke, R.A., 1992. Bioaccumulation of Pcbs from sediments by oligochaetes and fishes - comparison of laboratory and field studies. Can. J. Fish. Aquat. Sci. 49, 2080–2085.
Barnes, D.K.A., Galgani, F., Thompson, R.C., Barlaz, M., 2009. Accumulation and fragmentation of plastic debris in global environments. Philos T R Soc B 364, 1985–1998.
Batel, A., Linti, F., Scherer, M., Erdinger, L., Braunbeck, T., 2016. Transfer of benzo[a] pyrene from microplastics to Artemia nauplii and further to zebrafish via a trophic food web experiment: CYP1A induction and visual tracking of persistent organic pollutants. Environ. Toxicol. Chem. 35, 1656–1666.
Besseling, E., Foekema, E.M., van den Heuvel-Greve, M.J., Koelmans, A.A., 2017a. The effect of microplastic on the uptake of chemicals by the lugworm Arenicola marina (L.) under environmentally relevant exposure conditions. Environ Sci Technol 51, 8795–8804.
Besseling, E., Quik, J.T.K., Sun, M., Koelmans, A.A., 2017b. Fate of nano- and microplastic in freshwater systems: a modeling study. Environ. Pollut. 220, 540–548.
Bjorkland, R., Tobias, D.A., Petersen, E.J., 2017. Increasing evidence indicates low bioaccumulation of carbon nanotubes. Environ-Sci Nano 4, 747–766.
Caballero-Guzman, A., Nowack, B., 2016. A critical review of engineered nanomaterial release data: are current data useful for material flow modeling? Environ. Pollut. 213, 502–517.
Caballero-Guzman, A., Nowack, B., 2018. Prospective nanomaterial mass flows to the environment by life cycle stage from five applications containing CuO, DPP, FeOx, CNT and SiO2. J. Clean. Prod. 203, 990–1002.
Casado, M.P., Macken, A., Byrne, H.J., 2013. Ecotoxicological assessment of silica and polystyrene nanoparticles assessed by a multitrophic test battery. Environ. Int. 51, 97–105.
Cedervall, T., Hansson, L.A., Lard, M., Frohm, B., Linse, S., 2012. Food chain transport of nanoparticles affects behaviour and fat metabolism in fish. PLoS One 7.
Cena, L.G., Peters, T.M., 2011. Characterization and control of airborne particles emitted during production of epoxy/carbon nanotube nanocomposites. J. Occup. Environ. Hyg. 8, 86–92.
Chua, E.M., Shimeta, J., Nugegoda, D., Morrison, P.D., Clarke, B.O., 2014. Assimilation of Polybrominated diphenyl ethers from microplastics by the marine amphipod, Allorchestes Compressa. Environ Sci Technol 48, 8127–8134.
Cimbaluk, G.V., Ramsdorf, W.A., Perussolo, M.C., Santos, H.K., De Assi, H.C.S., Schnitzler, M.C., Schnitzler, D.C., Carneiro, P.G., Cestari, M.M., 2018. Evaluation of multiwalled carbon nanotubes toxicity in two fish species. Ecotox Environ Safe 150, 215–223.
Derraik, J.G.B., 2002. The pollution of the marine environment by plastic debris: a review. Mar. Pollut. Bull. 44, 842–852.
Duis, K., Coors, A., 2016. Microplastics in the aquatic and terrestrial environment: sources (with a specific focus on personal care products), fate and effects. Environ. Sci. Eur. 28.
Eckelman, M.J., Mauter, M.S., Isaacs, J.A., Elimelech, M., 2012. New perspectives on nanomaterial aquatic ecotoxicity: production impacts exceed direct exposure impacts for carbon nanotubes. Environ Sci Technol 46, 2902–2910.
Eerkes-Medrano, D., Thompson, R.C., Aldridge, D.C., 2015. Microplastics in freshwater systems: a review of the emerging threats, identification of knowledge gaps and prioritisation of research needs. Water Res. 75, 63–82.
Farre, M., Gajda-Schrantz, K., Kantiani, L., Barcelo, D., 2009. Ecotoxicity and analysis of nanomaterials in the aquatic environment. Anal. Bioanal. Chem. 393, 81–95.
Farrell, P., Nelson, K., 2013. Trophic level transfer of microplastic: Mytilus edulis (L.) to Carcinus maenas (L.). Environ. Pollut. 177, 1–3.
Gigault, J., ter Halle, A., Baudrimont, M., Pascal, P.Y., Gauffre, F., Phi, T.L., El Hadri, H., Grassl, B., Reynaud, S., 2018. Current opinion: what is a nanoplastic? Environ. Pollut. 235, 1030–1034.
Ging, J., Tejerina-Anton, R., Ramakrishnan, G., Nielsen, M., Murphy, K., Gorham, J.M., Nguyen, T., Orlov, A., 2014. Development of a conceptual framework for evaluation of nanomaterials release from nanocomposites: environmental and toxicological implications. Sci. Total Environ. 473, 9–19.
Glomstad, B., Zindler, F., Jenssen, B.M., Booth, A.M., 2018. Dispersibility and dispersion stability of carbon nanotubes in synthetic aquatic growth media and natural freshwater. Chemosphere 201, 269–277.
Gojny, F.H., Wichmann, M.H.G., Fiedler, B., Schulte, K., 2005. Influence of different carbon nanotubes on the mechanical properties of epoxy matrix composites - a comparative study. Compos. Sci. Technol. 65, 2300–2313.
Gottschalk, F., Kost, E., Nowack, B., 2013a. Engineered nanomaterials in water and soils: a risk quantification based on probabilistic exposure and effect modeling. Environ. Toxicol. Chem. 32, 1278–1287.
Gottschalk, F., Sun, T.Y., Nowack, B., 2013b. Environmental concentrations of engineered nanomaterials: review of modeling and analytical studies. Environ. Pollut. 181, 287–300.
Harper, S., Wohlleben, W., Doa, M., Nowack, B., Clancy, S., Canady, R., Maynard, A., 2015. Measuring nanomaterial release from carbon nanotube composites: review of the state of the science. 4th International Conference on Safe Production and Use of

Nanomaterials (Nanosafe2014) 617.
Hirth, S., Cena, L., Cox, G., Tomovic, Z., Peters, T., Wohlleben, W., 2013. Scenarios and methods that induce protruding or released CNTs after degradation of nanocomposite materials. J. Nanopart. Res. 15.
Hollertz, R., Chatterjee, S., Gutmann, H., Geiger, T., Nuesch, F.A., Chu, B.T.T., 2011. Improvement of toughness and electrical properties of epoxy composites with carbon nanotubes prepared by industrially relevant processes. Nanotechnology 22.
Hurley, R.R., Woodward, J.C., Rothwell, J.J., 2017. Ingestion of microplastics by freshwater Tubifex Worms. Environ Sci Technol 51, 12844–12851.
Ivleva, N.P., Wiesheu, A.C., Niessner, R., 2017. Microplastic in aquatic ecosystems. Angew Chem Int Edit 56, 1720–1739.
Jackson, P., Jacobsen, N.R., Baun, A., Birkedal, R., Kuhnel, D., Jensen, K.A., Vogel, U., Wallin, H., 2013. Bioaccumulation and ecotoxicity of carbon nanotubes. Chem Cent J 7.
Jackson, E.M., Laibinis, P.E., Collins, W.E., Ueda, A., Wingard, C.D., Penn, B., 2016. Development and thermal properties of carbon nanotube-polymer composites. Compos Part B-Eng 89, 362–373.
Jambeck, J.R., Geyer, R., Wilcox, C., Siegler, T.R., Perryman, M., Andrady, A., Narayan, R., Law, K.L., 2015. Plastic waste inputs from land into the ocean. Science 347, 768–771.
Kesy, K., Oberbeckmann, S., Muller, F., Labrenz, M., 2016. Polystyrene influences bacterial assemblages in Arenicola marina-populated aquatic environments in vitro. Environ. Pollut. 219, 219–227.
Kingston, C., Zepp, R., Andrady, A., Boverhof, D., Fehir, R., Hawkins, D., Roberts, J., Sayre, P., Shelton, B., Sultan, Y., Vejins, V., Wohlleben, W., 2014. Release characteristics of selected carbon nanotube polymer composites. Carbon 68, 33–57.
Koelmans, A.A., Besseling, E., Shim, W.J., 2015. Nanoplastics in the aquatic environment. Critical review. In: Bergmann, M., Gutow, L., Klages, M. (Eds.), Marine Anthropogenic Litter. Springer International Publishing, Cham, pp. 325–340.
Koivisto, A.J., Jensen, A.C.O., Kling, K.I., Norgaard, A., Brinch, A., Christensen, F., Jensen, K.A., 2017. Quantitative material releases from products and articles containing manufactured nanomaterials: towards a release library. Nanoimpact 5, 119–132.
Kooi, M., Besseling, E., Kroeze, C., van Wezel, A.P., Koelmans, A.A., 2018. Modeling the fate and transport of plastic debris in freshwaters: review and guidance. In: Wagner, M., Lambert, S. (Eds.), Freshwater Microplastics: Emerging Environmental Contaminants? Springer International Publishing, Cham, pp. 125–152.
Lechner, A., Keckeis, H., Lumesberger-Loisl, F., Zens, B., Krusch, R., Tritthart, M., Glas, M., Schludermann, E., 2014. The Danube so colourful: a potpourri of plastic litter outnumbers fish larvae in Europe's second largest river. Environ. Pollut. 188, 177–181.
Maes, H.M., Stibany, F., Giefers, S., Daniels, B., Deutschmann, B., Baumgartner, W., Schaffer, A., 2014. Accumulation and distribution of multiwalled carbon nanotubes in zebrafish (Danio rerio). Environ Sci Technol 48, 12256–12264.
Neubauer, N., Wohlleben, W., Tomovic, Z., 2017. Conductive plastics: comparing alternative nanotechnologies by performance and life cycle release probability. J. Nanopart. Res. 19.
Nguyen, T., Pellegrin, B., Mermet, L., Shapiro, A., Gu, X., Chin, J., 2009. Network aggregation of CNTs at the surface of epoxy/MWCNT composite exposed to UV radiation. Nanotech Conference & Expo 1, 90–93 2009. Technical Proceedings.
Nguyen, T., Petersen, E.J., Pellegrin, B., Gorham, J.M., Lam, T., Zhao, M.H., Sung, L.P., 2017. Impact of UV irradiation on multiwall carbon nanotubes in nanocomposites: formation of entangled surface layer and mechanisms of release resistance. Carbon 116, 191–200.
Nowack, B., Mitrano, D.M., 2018. Procedures for the production and use of synthetically aged and product released nanomaterials for further environmental and ecotoxicity testing. Nanoimpact 10, 70–80.
Nowack, B., David, R.M., Fissan, H., Morris, H., Shatkin, J.A., Stintz, M., Zepp, R., Brouwer, D., 2013. Potential release scenarios for carbon nanotubes used in composites. Environ. Int. 59, 1–11.
OECD, 1992. Test No. 203: Fish, Acute Toxicity Test.
OECD, 2007. Test No. 225: Sediment-Water Lumbriculus Toxicity Test Using Spiked Sediment.
Petersen, E.J., Huang, Q.G., Weber, W.J., 2008a. Bioaccumulation of radio-labeled carbon nanotubes by Eisenia foetida. Environ Sci Technol 42, 3090–3095.
Petersen, E.J., Huang, Q.G., Weber, W.J., 2008b. Ecological uptake and depuration of carbon nanotubes by Lumbriculus variegatus. Environ Health Persp 116, 496–500.
Petersen, E.J., Akkanen, J., Kukkonen, J., Weber, W.J., 2009. Bioaccumulation of radioactively labeled multiwalled carbon nanotubes by Daphnia magna. Abstr Pap Am Chem S 237.
Petersen, E.J., Lam, T., Gorham, J.M., Scott, K.C., Long, C.J., Stanley, D., Sharma, R., Liddle, J.A., Pellegrin, B., Nguyen, T., 2014. Methods to assess the impact of UV irradiation on the surface chemistry and structure of multiwall carbon nanotube epoxy nanocomposites. Carbon 69, 194–205.
Primpke, S., Imhof, H., Piehl, S., Lorenz, C., Loder, M., Laforsch, C., Gerdts, G., 2017. Environmental chemistry microplastic in the environment. Chem Unserer Zeit 51, 402–412.
R Core Team, 2017. R: A language and environment for statistical computing. R Foundation for Statistical Computing, Vienna, Austria. http://www.R-project.org/.
Redondo-Hasselerharm, P.E., Falahudin, D., Peeters, E.T.H.M., Koelmans, A.A., 2018. Microplastic effect thresholds for freshwater benthic macroinvertebrates. Environ Sci Technol 52, 2278–2286.
Rhiem, S., Riding, M.J., Baumgartner, W., Martin, F.L., Semple, K.T., Jones, K.C., Schaffer, A., Maes, H.M., 2015. Interactions of multiwalled carbon nanotubes with algal cells: quantification of association, visualization of uptake, and measurement of alterations in the composition of cells. Environ. Pollut. 196, 431–439.
Rhiem, S., Barthel, A.K., Meyer-Plath, A., Hennig, M.P., Wachtendorf, V., Sturm, H., Schaffer, A., Maes, H.M., 2016. Release of C-14-labelled carbon nanotubes from polycarbonate composites. Environ. Pollut. 215, 356–365.
da Rocha, A.M., Ferreira, J.R., Barros, D.M., Pereira, T.C.B., Bogo, M.R., Oliveira, S., Geraldo, V., Lacerda, R.G., Ferlauto, A.S., Ladeira, L.O., Pinheiro, M.V.B., Monserrat, J.M., 2013. Gene expression and biochemical responses in brain of zebrafish Danio rerio exposed to organic nanomaterials: carbon nanotubes (SWCNT) and fullerenol (C-60(OH)(18-22)(OK4)). Comp Biochem Phys A 165, 460–467.
Rochman, C.M., Hoh, E., Kurobe, T., Teh, S.J., 2013. Ingested plastic transfers hazardous chemicals to fish and induces hepatic stress. Sci Rep-Uk 3, 3263.
Rochman, C.M., Kurobe, T., Flores, I., Teh, S.J., 2014. Early warning signs of endocrine disruption in adult fish from the ingestion of polyethylene with and without sorbed chemical pollutants from the marine environment. Sci. Total Environ. 493, 656–661.
Schierz, A., Espinasse, B., Wiesner, M.R., Bisesi, J.H., Sabo-Attwood, T., Ferguson, P.L., 2014. Fate of single walled carbon nanotubes in wetland ecosystems. Environ-Sci Nano 1, 574–583.
Schlagenhauf, L., Buerki-Thurnherr, T., Kuo, Y.Y., Wichser, A., Nuesch, F., Wick, P., Wang, J., 2015a. Carbon nanotubes released from an epoxy-based nanocomposite: quantification and particle toxicity. Environ Sci Technol 49, 10616–10623.
Schlagenhauf, L., Kianfar, B., Buerki-Thurnherr, T., Kuo, Y.Y., Wichser, A., Nuesch, F., Wick, P., Wang, J., 2015b. Weathering of a carbon nanotube/epoxy nanocomposite under UV light and in water bath: impact on abraded particles. Nanoscale 7, 18524–18536.
Schwab, F., Bucheli, T.D., Lukhele, L.P., Magrez, A., Nowack, B., Sigg, L., Knauer, K., 2011. Are carbon nanotube effects on green algae caused by shading and agglomeration? Environ Sci Technol 45, 6136–6144.
Setala, O., Fleming-Lehtinen, V., Lehtiniemi, M., 2014. Ingestion and transfer of microplastics in the planktonic food web. Environ. Pollut. 185, 77–83.
Sulong, A.B., Park, J., Lee, N., Goak, J., 2006. Wear behavior of functionalized multiwalled carbon nanotube reinforced epoxy matrix composites. J. Compos. Mater. 40, 1947–1960.
Sun, T.Y., Gottschalk, F., Hungerbuhler, K., Nowack, B., 2014. Comprehensive probabilistic modelling of environmental emissions of engineered nanomaterials. Environ. Pollut. 185, 69–76.
Sun, T.Y., Bornhoft, N.A., Hungerbuhler, K., Nowack, B., 2016. Dynamic probabilistic modeling of environmental emissions of engineered nanomaterials. Environ Sci Technol 50, 4701–4711.
Sun, T.Y., Mitrano, D.M., Bornhoft, N.A., Scheringer, M., Hungerbuhler, K., Nowack, B., 2017. Envisioning Nano release dynamics in a changing world: using dynamic probabilistic modeling to assess future environmental emissions of engineered nanomaterials. Environ Sci Technol 51, 2854–2863.
Thompson, R.C., Olsen, Y., Mitchell, R.P., Davis, A., Rowland, S.J., John, A.W.G., McGonigle, D., Russell, A.E., 2004. Lost at sea: where is all the plastic? Science 304, 838.
Thompson, R.C., Swan, S.H., Moore, C.J., vom Saal, F.S., 2009. Our plastic age. Philos T R Soc B 364, 1973–1976.
Vilar, G., Fernandez-Rosas, E., Puntes, V., Jamier, V., Aubouy, L., Vazquez-Campos, S., 2013. Monitoring migration and transformation of nanomaterials in polymeric composites during accelerated aging. J. Phys. Conf. Ser. 429.
Watts, A.J.R., Lewis, C., Goodhead, R.M., Beckett, S.J., Moger, J., Tyler, C.R., Galloway, T.S., 2014. Uptake and retention of microplastics by the shore crab Carcinus maenas. Environ Sci Technol 48, 8823–8830.
Wetzel, B., Haupert, F., Zhang, M.Q., 2003. Epoxy nanocomposites with high mechanical and tribological performance. Compos. Sci. Technol. 63, 2055–2067.
Wohlleben, W., Brill, S., Meier, M.W., Mertler, M., Cox, G., Hirth, S., von Vacano, B., Strauss, V., Treumann, S., Wiench, K., Ma-Hock, L., Landsiedel, R., 2011a. On the lifecycle of nanocomposites: comparing released fragments and their in-vivo hazards from three release mechanisms and four nanocomposites. Small 7, 2384–2395.
Wohlleben, W., Ma-Hock, L., Treumann, S., van Ravenzwaay, B., Landsiedel, R., 2011b. Toxicological properties and possible release of MWCNT from composite materials. N-S Arch Pharmacol 383, 100.
Wohlleben, W., Meier, M.W., Vogel, S., Landsiedel, R., Cox, G., Hirth, S., Tomovic, Z., 2013. Elastic CNT-polyurethane nanocomposite: synthesis, performance and assessment of fragments released during use. Nanoscale 5, 369–380.
Wohlleben, W., Meyer, J., Muller, J., Muller, P., Vilsmeier, K., Stahlmecke, B., Kuhlbusch, T.A.J., 2016. Release from nanomaterials during their use phase: combined mechanical and chemical stresses applied to simple and multi-filler nanocomposites mimicking wear of nano-reinforced tires. Environ-Sci Nano 3, 1036–1051.
Wohlleben, W., Kingston, C., Carter, J., Sahle-Demessie, E., Vazquez-Campos, S., Acrey, B., Chen, C.Y., Walton, E., Egenolf, H., Muller, P., Zepp, R., 2017. NanoRelease: pilot interlaboratory comparison of a weathering protocol applied to resilient and labile polymers with and without embedded carbon nanotubes. Carbon 113, 346–360.
Wright, S.L., Rowe, D., Thompson, R.C., Galloway, T.S., 2013. Microplastic ingestion decreases energy reserves in marine worms. Curr. Biol. 23, R1031–R1033.